ASYMPTOTIC KULLBACK-LEIBLER INCREMENT TO CHARACTERIZE EXPERIMENT-INDUCED STRESS

Estelle Blons[†], *Eric Grivel*[**], *Véronique Deschodt-Arsac*[†] *and Véronique Lespinet-Najib*[**]

Bordeaux University[†] - INP Bordeaux[**] IMS - UMR CNRS 5218, Talence, FRANCE

ABSTRACT

In this paper, we first propose to analyze the properties of the Kullback-Leibler divergence between wide-sense stationary random processes that can be modeled by ARMA or ARFIMA processes. This study makes it possible to introduce a new feature useful to compare two random processes and called "the asymptotic KL increment". The latter depends on various parameters such as the inverse filters associated to the random processes. An interpretation of "the asymptotic KL increment" is also given. Then, we propose to use it in order to compare the inter-beat intervals, which characterize the cardiac rhythm, when the subjects are either in a calm and soothing situation or under stress.

***Index Terms*—** Kullback-Leibler divergence, asymptotic analysis, experiment-induced stress.

1. INTRODUCTION

Various works have been done on process comparison and statistical change detection. One of the authors recently focused his attention on the Jeffreys divergence (JD), which is the symmetric version of the Kullback-Leibler (KL) divergence, between the joint distributions of k consecutive samples of zero-mean autoregressive fractionally integrated with moving average process (ARFIMA) processes[1] [12] [11] [6] [13] [7] [18]. The analysis of the increment of the JD, *i.e.* the difference between two JDs computed for $k+1$ and k successive variates, when k increases, can be summarized as follows: after a transient behavior, the JD increment tends to a finite value called "asymptotic JD increment", except when the ARFIMA processes have different unit zeros and/or when the difference between the differencing orders of the ARFIMA processes is larger than $\frac{1}{2}$. In these particular cases, the limit of the increment tends to infinity. The asymptotic JD increment between zero-mean ARFIMA processes can be interpreted as follows: It consists in calculating the power of the first process filtered by the so-called inverse filter associated with the second one, and conversely. This explains the atypical cases where the asymptotic JD increments tend to infinity.

Nevertheless, the authors were asked about the expression of the asymptotic JD increment when dealing with non-zero mean processes. In addition, some colleagues wondered whether the behavior of the KL was similar since there is an additional term depending on the logarithm of the determinants of the covariance matrices of the processes. Finally, this approach was only used with synthetic data. For the above three reasons, our contribution in this paper is twofold:

1/ we propose to analyze the KL divergence between the joint distributions of k consecutive samples of random processes, which are non necessarily zero-mean and the PSD of which is continuous and can be null for a finite number of frequencies. In addition, the processes can be short or long memory. An analytical expression of the asymptotic KL increment is also provided by using the partial correlation coefficients (PACF) of the processes.

2/ we suggest considering the asymptotic KL increment to compare inter-beat intervals (*i.e.* RR-intervals). These biomarkers are usually useful to analyze the heart rate variability. In this paper, they are recorded during experiments the purpose of which is to analyze the experiment-induced stress and its effect on the cardiac autonomic nervous system. It should be noted that this work is done within a multidisciplinary project gathering psychologists, physiologists and researchers working in the field of signal processing.

The remainder of this paper is organized as follows: In section 2, some statistical properties of ARMA and ARFIMA processes are recalled. In section 3, a theoretical analysis of the evolution of the KL shows that the asymptotic KL increment can be of interest to compare different processes with respect to a reference process. In section 4, this approach is respectively used to illustrate the theory with synthetic data and to analyze inter-beats intervals recorded from Polar H10 heart rate belts in order to evaluate the experiment-induced stress effects on the cardiac autonomic nervous system. It is used with some traditional measures that are considered by the physiologists such as the root mean square of successive differences (RMSSD) [15], the ratio of powers in low and high frequencies [15], the multi-scale entropy (MSE) [4], the detrended fluctuations analysis (DFA) [17] and the detrended moving average method (DMA) [1].

[1]Note that an ARMA process with orders (p, q) corresponds to an ARFIMA process with orders (p, q) and a differencing order d equal to 0.

2. ABOUT ARMA AND ARFIMA PROCESSES

The wide-sense stationary (w.s.s.) ARMA process x_k can be seen as the output of a linear filter whose input u_k is a white noise process with variance σ_u^2 and whose transfer function denoted as $H(z)$ is rational. In addition, as the correlation function, r_τ with τ the lag, geometrically decays to zero, $\sum r_\tau$ is absolutely summable and this process is a short-memory process. In various applications such as economics, the values of the correlation function tend to decay to zero at a slower rate. This leads to long-memory processes for which $\sum r_\tau$ is no longer finite. This family includes the AR fractionally integrated MA (ARFIMA) processes [16]. Let us define it from the z-transforms of the process itself and the driving process:

$$X(z) = \frac{\prod_{l=1}^{q}(1-z_l z^{-1})}{\prod_{l=1}^{p}(1-p_l z^{-1})(1-z^{-1})^d}U(z) = H(z)U(z) \tag{1}$$

where $\{p_l\}_{l=1,\dots,p}$ are the non-unit poles and $\{z_l\}_{l=1,\dots,q}$ are the zeros. In addition, the differencing order d plays a role on the high-lag correlation structure. When $(p,q)=(0,0)$, this leads to fractionally integrated $FI(d)$ white noise. When $d > \frac{1}{2}$, the process is non-stationary and has an infinite variance. If $0 < d < \frac{1}{2}$, it exhibits long memory or persistence, whereas it has intermediate memory when $-\frac{1}{2} < d < 0$.

Finally, let us define the inverse filter. When all the zeros are inside the unit-circle in the z-plane, $H(z)$ is minimum-phase and directly invertible. However, when a zero has its modulus larger than 1, the following transformation can be considered:

$$H_{z_l}(z) = (1-z_l z^{-1}) = -z_l^* H_{bla,z_l}^{-1}(z)\left(1-\frac{1}{z_l^*}z^{-1}\right) \tag{2}$$

where z_l^* is the conjugate of z_l, $H_{bla,z_l}(z) = \frac{z^{-1}-z_l^*}{1-z_l z^{-1}}$ is a Blaschke product [3] up to a multiplicative value of the form $\pm e^{j\phi_l}$ with ϕ_l the argument of z_l. (2) amounts to saying that $H_{z_l}(z)$ can be expressed as the product of three transfer functions which correspond to two all-pass filters with gains respectively equal to $|z_l|$ and 1 and a minimum-phase filter. Note that the gain $|z_l|$ could be rather incorporated in the characterization of the filter input, by multiplying the variance of the driving process by $K_l = |z_l|^2$. This remark will be useful in subsection B. 2). Therefore, the BIBO-stable inverse filter is defined as follows:

$$H^{-1}(z) = \frac{1}{\sigma_u}\prod_{l=1}^{p}(1-p_l z^{-1})(1-z^{-1})^d \prod_{l=1}^{q} H_{z_l}^{-1}(z) \tag{3}$$

with

$$H_{z_l}^{-1}(z) = \begin{cases} \frac{1}{1-z_l z^{-1}} \text{ if } |z_l|<1 \\ \frac{1}{-z_l *}\frac{1}{1-\frac{1}{z_l^*}z^{-1}} \text{ if } |z_l|>1 \end{cases} \tag{4}$$

In this section, the driving process, and consequently the process, was assumed to be zero-mean. However, in practice, the processes are not necessarily zero-mean and can correspond to the sum of a constant and a zero-mean ARFIMA process. Therefore, in the next section, we suggest comparing non-zero mean Gaussian random processes by using the KL.

3. ABOUT KULLBACK-LEIBLER DIVERGENCE

Let us first recall that the probability distribution function (pdf) of the i^{th} real random Gaussian vector of size k, mean $\mu_{k,i}$ and covariance matrix $Q_{k,i}$, is defined by:

$$p_i(X_{k,i}) = \frac{1}{(\sqrt{2\pi})^k|Q_{k,i}|^{1/2}}\times \\ exp\Big(-\frac{1}{2}[X_{k,i}-\mu_{k,i}]^T Q_{k,i}^{-1}[X_{k,i}-\mu_{k,i}]\Big) \tag{5}$$

with $X_{k,i}$ the column vector storing k first values of the i^{th} process and $|Q_{k,i}|$ the determinant of the covariance matrix.
To study the dissimilarities between two pdfs [10], the KL divergence is given by:

$$KL_k^{(1,2)} = \int_{x_{1:k}} p_1(x_{1:k})\ln\left(\frac{p_1(x_{1:k})}{p_2(x_{1:k})}\right)\mathrm{d}x_{1:k} \tag{6}$$

Let $Tr(.)$ be the trace. By substituting the pdfs by (5), it can be shown that the KL satisfies:

$$KL_k^{(1,2)} = \frac{1}{2}\Big[\mathrm{Tr}(Q_{k,2}^{-1}Q_{k,1}) - k - \ln\frac{|Q_{k,1}|}{|Q_{k,2}|} \\ + \mathrm{Tr}(Q_{k,2}^{-1}(\mu_{k,2}-\mu_{k,1})(\mu_{k,2}-\mu_{k,1})^T)\Big] \tag{7}$$

Several issues can occur when the divergences are used in practice. Among the questions that can be considered, one can wonder which value of k must be chosen. In the following, our purpose is to see how to address this problem. More particularly, let us study the expression of $KL_k^{(1,2)}$, especially when k increases. We will see that the increment of the KL, *i.e.* $\Delta KL_k^{(1,2)} = KL_{k+1}^{(1,2)} - KL_k^{(1,2)}$, tends to a constant in most of the cases. Therefore, using the so-called asymptotic increment of the KL is of interest. Given (7) and introducing $\Delta\mu_k = \mu_{k,2}-\mu_{k,1}$, one has:

$$\Delta KL_k^{(1,2)} = \frac{1}{2}\big(\mathrm{Tr}(Q_{k+1,2}^{-1}Q_{k+1,1}) - \mathrm{Tr}(Q_{k,2}^{-1}Q_{k,1}) - 1\big) \\ + \frac{1}{2}\Big(\mathrm{Tr}\big(Q_{k+1,2}^{-1}\Delta\mu_{k+1}\Delta\mu_{k+1}^T\big) - \mathrm{Tr}\big(Q_{k,2}^{-1}\Delta\mu_k\Delta\mu_k^T\big)\Big) \\ - \frac{1}{2}\ln\Big(\frac{|Q_{k+1,1}|}{|Q_{k,1}|}\frac{|Q_{k,2}|}{|Q_{k+1,2}|}\Big) \tag{8}$$

The above expression (8) consists of three terms we analyze in the remainder of the section. Let us express the correlation matrices by using their eigenvalues and eigenvectors, with $i = 1, 2$:

$$Q_{k,i} = E\left[X_{k,i}X_{k,i}^T\right] = P_{k,i}D_{k,i}P_{k,i}^T \tag{9}$$

where $P_{k,i}$ denotes the unitary matrix storing the k eigenvectors of $Q_{k,i}$ and $D_{k,i}$ is the diagonal matrix defined with the k non-null real positive eigenvalues.

Pre-multiplying $X_{k,1}$ by $D_{k,1}^{-1/2}P_1^T$ consists in whitening the process vector. As the process is assumed to be w.s.s. and when k tends to infinity, this amounts to filtering all the samples stored in $X_{k,1}$ by the inverse filter defined by the transfer function $H_1^{-1}(z)$. Similarly, pre-multiplying $X_{k,1}$ by $D_{k,2}^{-1/2}P_{k,2}^T$ amounts to filtering the vector $X_{k,1}$ by the inverse filter $H_2^{-1}(z)$. Therefore, the limit of the first term in

(8) can be expressed as a function of the power $P^{(1,2)}$ of the 1^{st} process filtered by $H_2^{-1}(z)$ as follows:

$$\lim_{k\to+\infty} \frac{1}{2}\left(\text{Tr}(Q_{k+1,2}^{-1}Q_{k+1,1}) - \text{Tr}(Q_{k,2}^{-1}Q_{k,1}) - 1\right) \tag{10}$$
$$= \frac{1}{2}(P^{(1,2)} - 1)$$

For the second term in (8), as the processes are w.s.s., their means are constant and the vectors $\mu_{k,1}$ and $\mu_{k,2}$ store k times the same value μ_1 and μ_2 respectively. Therefore, one has:

$$\lim_{k\to+\infty} \frac{1}{2}\Big(Tr\big(Q_{k+1,2}^{-1}\Delta\mu_{k+1}\Delta\mu_{k+1}^T\big) - Tr\big(Q_{k,2}^{-1}\Delta\mu_k\Delta\mu_k^T\big)\Big) \tag{11}$$
$$= \frac{(\mu_1-\mu_2)^2}{2}|H_2^{-1}(z)|^2_{z=0}$$

Let us now look at third term in (8). Taking into account the link between the covariance matrices and the normalized-covariance matrices, *i.e.* $C_{k+1,i} = \frac{1}{r_{0,i}}Q_{k+1,i}$ for $i = 1, 2$, one has:

$$\frac{|Q_{k+1,1}||Q_{k,2}|}{|Q_{k,1}||Q_{k+1,2}|} = \frac{r_{0,1}}{r_{0,2}}\frac{|C_{k+1,1}|}{|C_{k,1}|}\frac{|C_{k,2}|}{|C_{k+1,2}|} \tag{12}$$

However, the determinant of the normalized-covariance matrices can be expressed from the PACF[2] $\phi_{\tau,i}$ with $i = 1, 2$:

$$|C_{k+1,i}| = |C_{k,i}|\prod_{\tau=1}^{k}(1-\phi_{\tau,i}^2) \tag{13}$$

Depending on the random processes under study, the PACF can become equal to 0 or not. Indeed, for a p^{th}-order AR process, the PACFs are equal to 0 for $\tau > p$ and non-zero for the other positive values. When dealing with MA processes, the PACF are all non-null since the MA processes can be seen as AR(∞) processes. They however tend to zero when the lag τ tends to infinity. Thus, for a MA(1) process, it can be shown that $\phi_{\tau,i}$ can be expressed from the MA parameter $b_{1,i}$:

$$\phi_{\tau,i} = \frac{(-1)^{\tau+1}b_{1,i}^\tau}{1 + b_{1,i}^2 + b_{1,i}^4 + ... + b_{1,i}^{2\tau}} \tag{14}$$

Concerning a FI process, the PACF depend on the differencing order d_i and are equal to $\frac{d_i}{\tau-d_i}$ [16]. More generally, for a w.s.s. ARFIMA process with $0 < d_i < \frac{1}{2}$, they are approximately equal to $\frac{d_i}{\tau}$ when τ tends to infinity [9]. Therefore, whatever the type of process, the limit of the ratio between the determinants of the covariance matrices tends to a constant denoted L_i:

$$\lim_{k\to+\infty}\frac{|C_{k+1,i}|}{|C_{k,i}|} = \lim_{k\to+\infty}\prod_{\tau=1}^{k}(1-\phi_{\tau,i}^2) = L_i = Cte \tag{15}$$

As the squares of the reflexion coefficients and the PACF are necessarily equal, one can use the way the variance of the driving process is updated with the Durbin-Levinson algorithm [14] to express the constant L_i from the variance of the driving process of the i^{th} process. Indeed, one has:

$$\lim_{k\to+\infty} r_{0,i}\prod_{\tau=1}^{k}(1-\phi_{\tau,i}^2) = L_i r_{0,i} = \sigma_{u,i}^2\prod_{l=1}^{q_i}K_{l,i} \tag{16}$$

with $K_{l,i} = 1$ when the zero $z_{l,i}$ of the i^{th} process is inside the unit circle and $K_{l,i} = |z_{l,i}|^2$ when it is outside the unit-circle. This difference between both cases is due to (2).

Therefore, there is necessarily a finite limit for $\frac{|Q_{k+1,1}||Q_{k,2}|}{|Q_{k,1}||Q_{k+1,2}|}$ when k increases. Using (12), (15) and (16), one has:

$$\lim_{k\to+\infty}\frac{|Q_{k+1,1}||Q_{k,2}|}{|Q_{k,1}||Q_{k+1,2}|} = \frac{\sigma_{u,1}^2\prod_{l=1}^{q_1}K_{l,1}}{\sigma_{u,2}^2\prod_{l=1}^{q_2}K_{l,2}} \tag{17}$$

Given (10), (11), (12) and (17), the asymptotic KL increment satisfies:

$$\Delta KL^{(1,2)} = \lim_{k\to+\infty}\Delta KL_k^{(1,2)} = \frac{1}{2}(P^{(1,2)} - 1) \tag{18}$$
$$+ \frac{(\mu_1-\mu_2)^2}{2}|H_2^{-1}(z)|^2_{z=0} - \frac{1}{2}\ln\frac{\sigma_{u,1}^2\prod_{l=1}^{q_1}K_{l,1}}{\sigma_{u,2}^2\prod_{l=1}^{q_2}K_{l,2}}$$

For short-memory processes like ARMA processes, the only reason for which this asymptotic increment could not be finite is the fact that the transfer function associated to the second process has a zero on a unit-circle in the z-plane that is not shared with the transfer function associated to the first process. For FI and ARFIMA processes, there may be other reasons: if the modulus of the difference between two differencing orders is larger than $\frac{1}{2}$, the process that is obtained after inverse filtering has an infinite power.

Remark: Jeffreys divergence (JD) is defined as $\frac{1}{2}(KL_k^{(1,2)} + KL_k^{(2,1)})$. Using (18), the expression of the asymptotic JD increment for zero-mean processes used in [7] can be retrieved.

4. ILLUSTRATIONS

4.1. With synthetic data

Let us compare two MA processes whose orders are respectively equal to 4 and 6. The zeros are set to 2, $-1/3$ and $0.9e^{\pm j\pi/3}$ for the first and 2, $-1/5$, $0.5e^{\pm j\pi/4}$ and $3e^{\pm j\pi/5}$ for the second. The variances are equal to 1.

The asymptotic KL increment is estimated using a realization of each process based on $N = 10000$ samples as follows: the covariance matrices and the means are estimated by using a maximum-likelihood estimator for different sizes k in an interval k_{min} and k_{max} defined by the practitioner. Then, the increments are computed. Due to the convergence to (18), the differences between two consecutive increments tend to zero. Therefore, once these differences are smaller than a predefined threshold, the KL increments are averaged to get an estimation of the asymptotic KL increment. Fig. 1 confirms that the KL increment converges to the limit defined in (18).

[2] After expressing the i^{th} process at times k and $k-\tau$ as linear combinations of the τ values $x_{k-1,i}, .., x_{k-\tau+1,i}$ and their residuals, the PACF $\phi_{\tau,i}$ is defined as the correlation coefficient computed between both residuals. Its modulus is hence necessarily in the interval $[0, 1]$. Up to a multiplication by ± 1, the PACF corresponds to the reflexion coefficient.

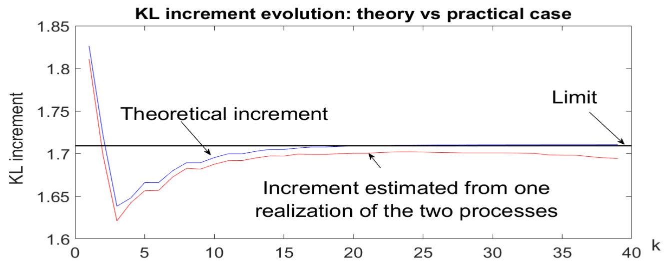

Fig. 1: Illustration confirming the theoretical analysis

4.2. Analyzing RR intervals to study experiment-induced stress

Several studies show that the cognitive tasks and the stress induced by the experiment involves the central nervous system. Studies using RR intervals have been recently led to analyze the interconnections between cardiac regulations and central nervous system [2] [5] [20]. Therefore, we developed a psychological protocol aiming at inducing several levels of stress during a cognitive task. The levels of experiment-induced stress and workload were controlled with questionnaires validated in psychology [8] [19].

Four situations were considered for this experiment, during which the subjects were seated in front of a computer in a room at 20°C between 10 am and noon in order to limit the effects of chronobiology: a reference situation (Ref), a situation of cognitive tasks (T_c), and two situations of cognitive tasks associated to an experiment-induced stress: a small level of stress ($T_c + S_1$) and a high one ($T_c + S_2$). During Ref, the subjects watched a calm and soothing documentary during 10 min. Then, during the three other situations, the subjects had to remain silent and 23, 28 and 31 questions of logic, memorization and mental calculation were asked. During $T_c + S_1$ and $T_c + S_2$, negative visual feedbacks appeared in false responses to amplify the experiment-induced stress. Both situations differed in the following manner: during $T_c + S_1$, all the questions had to be completed in a limited time of 7 minutes. During $T_c + S_2$, each question was displayed for a predefined time, not controllable by the subject. Two people were near the subject and behave as an attentive and evaluative audience. Sound disturbances were also added.

There were 25 subjects (12 women and 13 men, 27.8 $\pm$ 7.8 years). Each protocol took 1.5 hour.

Cardiac autonomic markers were assessed from recorded RR intervals for 7 to 10 min, depending on the experimental situations, by using a Polar H10 belt associated by Bluetooth with the application HRV Logger.

Usually, RMSSD [15], the ratio of powers in low and high frequency (LF/HF) [15] are considered. The MSE is also computed by using [4]. In addition, the Hurst exponent, denoted as H, which characterizes the degree of long-range dependence, is estimated by using the DFA [17]. It operates with the following steps: the signal is first integrated and split into segments. Local trends are deduced. The resulting piecewise linear trend is subtracted to the whole signal. The power of the residual is computed for different segment lengths. Then, the log-log representation corresponds to a straight line with a slope, denoted as α. Due to the integration of the signal, the slope is not directly equal to H but is equal to $H + 1$. As the trend of a process can be estimated with different manners, variants exist. Thus, for the DMA, the global trend is deduced by means of a finite-impulse response (FIR) low-pass filter. See [1].

As the asymptotic KL increment is computed between the RR intervals in the different situations and the one in Ref, we suggest computing the difference between the RMSSD, the LF/HF ratio, the MSE, the long-range DFA and the DMA estimated in the different situations and the ones obtained in Ref. They are denoted $\delta RMSSD$, etc. Their means and their standard deviations (std) based on the 25 subjects are given in Table 1. The stds are comparatively large since the physiological regulations depend on the individual characteristics. This is common in this type of experiment. Nevertheless, the evolutions of the features from Tc to $T_c + S_2$ for each subject are similar to the evolution of the mean.

Table 1: Different features. $RMSSD_{(Ref)} = 39 \pm 18$ ms, $LF/HF_{(Ref)} = 1.1 \pm 0.6$, $DFA_{(Ref)} = 0.84 \pm 0.17$, $DMA_{(Ref)} = 0.84 \pm 0.16$ and $MSE_{(Ref)} = 3.74 \pm 0.61$.

Features	Ref	T_c	$T_c + S_1$	$T_c + S_2$
$\delta RMSSD$	0	9 $\pm$12	6 $\pm$11	7 $\pm$11
$\delta LF/HF$	0	0.14 $\pm$0.34	0.20 $\pm$0.40	0.13 $\pm$0.38
δDFA	0	0.03 $\pm$0.17	-0.02 $\pm$0.17	0.09 $\pm$0.24
δDMA	0	0.02$\pm$0.16	-0.03 $\pm$0.15	0.09 $\pm$0.22
δMSE	0	0.32 $\pm$0.59	0.33 $\pm$0.53	0.22 $\pm$0.65
ΔKL	0	0.23 $\pm$0.19	0.22 $\pm$0.16	0.28 $\pm$0.27

Given Table 1, RMSSD and the ratio LF/HF are not able to distinguish the high level of stress $T_c + S_2$ from the other situations. However, the ratio LF/HF could be relevant to discriminate $T_c + S_1$ from T_c. This could be explained by the fact that these features are known to be related to the sympatho-vagal balance [15]. δMSE, δDMA and δDFA make it possible to point out the high level of stress $T_c + S_2$. The regularity of the RR intervals is probably modified due to the stress. Like δMSE, δDMA and δDFA, ΔKL also allow $T_c + S_2$ to be distinguished from the others.

Therefore, the ratio LF/HF and one of these three features could be combined to describe the different physiological and psychological states.

5. CONCLUSIONS AND PERSPECTIVES

The asymptotic KL increment can be used to compare random processes. It is also of interest to characterize a high level of stress. We plan to combine it with the standard features in order to classify subjects within a group in a crisis situation.

6. REFERENCES

[1] E. Alessio, A. Carbone, G. Castelli, and V. Frappietro. Second-order moving average and scaling of stochastic time series. *The European Physical Journal B - Condensed Matter and Complex Systems*, 27, 2:197200, 2002.

[2] S.J. Bishop. Neurocognitive mechanisms of anxiety: an integrative account. *Trends in Cognitive Sciences*, 11, no. 7, 2007.

[3] P. Colwell. *Blaschke products: bounded analytical functions*. University of Michigan Press, 1985.

[4] M. Costa, A. L. Goldberger, and C.-K. Peng. Multiscale entropy analysis of complex physiologic time series. *Physical Review Letters*, 89, 2002.

[5] D.A. Dimitriev, E.V. Saperova, and A.D. Dimitriev. State anxiety and nonlinear dynamics of heart rate variability in students. *Plos one*, 2016.

[6] E. Grivel, M. Saleh, and S.-M. Omar. Comparing a complex-valued sinusoidal process with an autoregressive process using Jeffreys divergence. *EUSIPCO*, 2017.

[7] E. Grivel, M. Saleh, and S.-M. Omar. Interpreting the asymptotic increment of Jeffrey's divergence between some random processes. *Elsevier Digital Signal Processing*, 75, (4):120–133, 2018.

[8] S. G. HartLowell and E. Staveland. Development of nasa-tlx (task load index): Results of empirical and theoretical research. *Advances in Psychology*, 52:139–183, 1988.

[9] A. Inoue. Asymptic behaviour for partial autocorrelation functions of fractionnal arima processes. *The Annals of Applied Probability*, 12:1471–1491, April 2002.

[10] S. Kullback and R. A. Leibler. On Information and Sufficiency. *The Annals of Mathematical Statistics*, 22, no. 1:79–86, 1951.

[11] L. Legrand and E. Grivel. Jeffrey's divergence between moving-average and autoregressive models. *IEEE ICASSP*, 2017.

[12] L. Legrand and E. Grivel. Jeffrey's divergence between moving-average models that are real or complex, noise-free or disturbed by additive white noises. *Elsevier Signal Processing*, 131:350–363, 2017.

[13] L. Legrand and E. Grivel. Jeffreys divergence between autoregressive processes disturbed by additive white noises. *Elsevier Signal Processing*, 149:162–178, 2018.

[14] M. Najim. *Modeling, estimation and optimal filtering in signal processing*. Wiley, 2010.

[15] Task Force of the European Society of Cardiology, the North American Society of Pacing, and Electrophysiology. Heart rate variability. standards of measurement, physiological interpretation, and clinical use. *European Heart Journal*, 17:354–381, 1996.

[16] W. Palma. *Long-Memory Time Series, Theory and Methods*. Wiley, 2007.

[17] C. K. Peng, S. V. Buldyrev, S. Havlin, M. Simons, H.E. Stanley, and A.L. Goldberger. Mosaic organization of DNA nucleotides. *Physical Review E*, 49, (2):1685–1689, 1994.

[18] M. Saleh, E. Grivel, and S.-M. Omar. Jeffrey's divergence between arfima processes. *Digital Signal Processing*, 82:175–186, 2018.

[19] C.D. Spielberger, R.L. Gorsuch, R. Lushene, and P.R. Vagg.

[20] H. Young and D. Benton. We should be using nonlinear indices when relating heart-rate dynamics to cognition and mood. *Scientific Reports*, 5, 2015.